

Organic & Biomolecular Chemistry

Accepted Manuscript



This is an *Accepted Manuscript*, which has been through the Royal Society of Chemistry peer review process and has been accepted for publication.

Accepted Manuscripts are published online shortly after acceptance, before technical editing, formatting and proof reading. Using this free service, authors can make their results available to the community, in citable form, before we publish the edited article. We will replace this *Accepted Manuscript* with the edited and formatted *Advance Article* as soon as it is available.

You can find more information about *Accepted Manuscripts* in the [Information for Authors](#).

Please note that technical editing may introduce minor changes to the text and/or graphics, which may alter content. The journal's standard [Terms & Conditions](#) and the [Ethical guidelines](#) still apply. In no event shall the Royal Society of Chemistry be held responsible for any errors or omissions in this *Accepted Manuscript* or any consequences arising from the use of any information it contains.

Cite this: DOI: 10.1039/c0xx00000x

www.rsc.org/xxxxxx

ARTICLE TYPE

Alkyl chain substituted 1, 9- Pyrazoloanthrones exhibit prominent inhibitory effect on c-Jun N-terminal Kinase (JNK).†

Karothu Durga Prasad,^a Jamma Trinath,^b Ansuman Biswas,^c Kanagaraj Sekar,^{*d} Kithiganahalli N. Balaji^{*#b} and Tayur N. Guru Row^{*#a}

5

N-alkyl substituted pyrazoloanthrone derivatives were synthesized, characterized and tested for their *in vitro* inhibitory activity over c-Jun N-terminal kinase (JNK). Among the tested molecules, a few derivatives showed significant inhibitory activity against JNK with minimal off-target effect on other mitogen-activated protein kinase (MAPkinase) family members such as MEK1/2 and MKK3,6. These results suggested that N-alkyl (propyl and butyl) bearing pyrazoloanthrone scaffolds provide promising therapeutic inhibitors for JNK in regulating inflammation associated disorders.

1. Introduction

Cellular physiological processes are critically tailored by numerous signalling pathways. Regulated activation of Mitogen Activated Protein Kinase (MAPkinase) family members determine the extent of mammalian gene expression.¹ Lipopolysaccharide (LPS), chief constituent of endotoxin, is the major cause of sepsis. Endotoxin mediated septic shock is mainly characterised by drastic and sudden augmentation of several inflammatory genes like IL-12, IL-1 β , TNF- α .² Exaggerated levels of these cytokines derails the host immune homeostasis leading to inflammation associated risks like cardiac arrest, arthritis, etc.³ Activation of host cellular signalling pathways comprised of MAP Kinases such as ERK 1/2, p38 and JNK predominantly, at the ground level is the key regulatory step in fine tuning the immune cell associated functions.^{4, 5} Design and characterization of novel small molecules on one hand and potentiating the exiting target specific inhibitors on the other attains crucial importance in the treatment of inflammation associated disorders.⁶⁻⁸ JNK (Jun N-terminal Kinase), a stress activated protein kinase (SAPK), is one of the important member of MAP kinase family along with MEK 1/2, MEK 3,6 and MKK 4,7, etc that mediates the activation of key transcription factor AP-1 (Activator Protein-1 complex composed of c-Fos and c-Jun).⁹⁻¹³ Activated JNK phosphorylates c-Jun at Ser 63 position and eventually leads to formation of a functional AP-1 transcription factor complex.^{14,15} Till date, three JNKs were identified in humans (JNK1, JNK2 and JNK3). In addition to these, 10 subsidiary isoforms arise from these JNK's as splice variants.¹⁶ JNK's with several isoformic variants control crucial cellular processes like apoptosis and cell proliferation and are also implicated in disorders associated with inflammation like septic shock, arthritis, inflammatory bowel disease, etc.^{17, 18} Therapeutic inhibition of JNK activity by small molecule inhibitors has proven to be advantageous in the treatment of diseases coupled with derailed inflammation.^{19, 20}

Even though, several inhibitors of JNK have already been reported²¹⁻²³ with varied efficacies, the role of anthracyclines identified in the screening of anti-cancer drugs²⁴ has not been focused in terms of kinase inhibitors until the introduction of 1, 9- Pyrazoloanthrone (SP600125) by Brydon *et al.*¹⁹ SP600125, a flat molecule²⁵ with free NH group in the pyrazole ring acts as a reversible ATP competitive inhibitor and has proved to be a small molecule inhibitor of JNK among several tested kinases.²⁶⁻²⁸ But the methyl and ethyl derivatives of pyrazoloanthrone exhibited loss of inhibitory activity¹⁹ and hence

other higher alkyl derivatives were not tested. From a chemistry perspective, the tautomerism in 1, 9-pyrazoloanthrone (anthra[1,9-c,d]pyrazol-6-one, **Fig. 1a**) was confirmed by the existence of two positional isomers after alkylation (**Fig. 1b**).²⁹ According to Scapin and co-workers³⁰, the crystal structure of JNK3 with 1,9-pyrazoloanthrone (PDB code: 1PMV) showed higher selectivity towards inhibition compared to the other molecules. It was shown that, SP600125 interacts with the protein via hydrogen bonds with the carbonyl oxygen of Glu147 and the main chain nitrogen of Met149. In addition, several hydrophobic contacts with Ile70, Ala91, Met146, Leu148, Asp150, Asn152, Val196 and Leu206 (**Fig. 1c**) are identified in the enzyme – inhibitor complex.

In this context, it may be surmised that increase in the alkyl chain length on nitrogen atom might invoke additional hydrophobic contacts in the active site of JNK, a feature which needs to be explored. In the present study the tautomerism in 1, 9-pyrazoloanthrone was substantiated by the positional isomers of alkyl derivatives and the structures have been established by single crystal X-ray diffraction studies. Based on calculated binding abilities with JNK structure generated from the *in silico* screening, 10 molecules were selected for initial screening of their kinase inhibitory activity. Among the tested molecules, a few of them show specific inhibition of JNK among the several MAP Kinases with favourable concentrations in the range of 1-20 μ M. These molecules deserve further evaluation in terms of their pharmacokinetic properties as well as biological functions to be potent therapeutics in resolving inflammation.

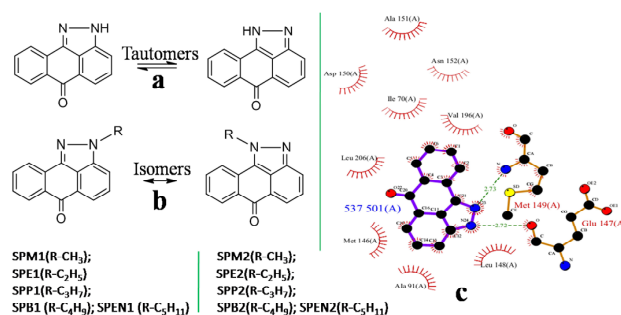


Fig. 1a and **1b** Chemical structures of 1,9-pyrazoloanthrone and N-alkylated pyrazoloanthrones. **Fig. 1c** Ligplot representation of interactions in the active site of JNK3 with SP600125 (1PMV).

2. Results and discussion

2.1 Synthesis

Based on preliminary results obtained with pyrazoloanthrones in *in silico* screening, *N*-alkyl substituted pyrazoloanthrones were synthesized according to modified procedures (ESI†). The compounds were characterized by ¹H & ¹³C NMR, HR-MS and the purity was assessed by the analytical HPLC method and found to be >98%. Crystal structures of these compounds were determined by single crystal X-ray diffraction.

2.2. Crystal structure determination

Substitution of alkyl group on pyrazole ring in 1,9-pyrazoloanthrone forms two isomers. For example, two isomers of the butyl derivative of 1, 9-pyrazoloanthrone (designated as **SPB1** and **SPB2**) were crystallized from a mixture of 30% EtOAc: hexane and their crystal structures were determined (Fig. 2; Table 1). Similarly, several alkyl derivatives of pyrazoloanthrone (**SPM1**, **SPE2**, **SPP1** and **SPP2**; ESI†) were crystallized by slow evaporation at ambient temperatures and their crystal structures were determined.

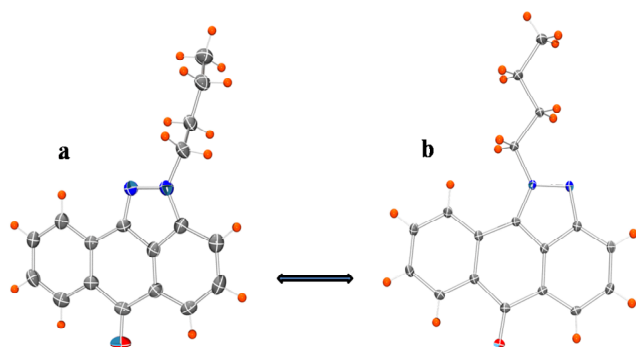


Fig. 2(a) and 2(b) ORTEP diagram of **SPB1** and **SPB2** with 50% probability displacement ellipsoids respectively.

Table 1 Crystallographic data for compounds **SPB1** and **SPB2**.

| Compound | SPB1 | SPB2 |
|---|---|--|
| Formula | C ₁₈ H ₁₆ N ₂ O | C ₁₈ H ₁₆ N ₂ O |
| Formula weight | 276.3324 | 276.3324 |
| system | Orthorhombic | Monoclinic |
| Space group | <i>P</i> 2 ₁ 2 ₁ 2 ₁ | <i>P</i> 2 ₁ / <i>c</i> |
| a (Å) | 4.909(5) | 4.933(2) |
| b (Å) | 14.694(2) | 15.036(7) |
| c (Å) | 19.031(2) | 18.387(9) |
| α | 90 | 90 |
| β | 90 | 91.93(5) |
| γ | 90 | 90 |
| Volume (Å ³) | 1372.93(3) | 1363.07(2) |
| Z | 4 | 4 |
| Density (gcm ⁻³) | 1.34 | 1.35 |
| μ (mm ⁻¹) | 0.084 | 0.085 |
| F (000) | 583.9 | 583.9 |
| No. of measured reflections | 9877 | 21681 |
| No. of unique reflections | 3001 | 2671 |
| No. of reflections used | 1861 | 2173 |
| R _{all} , R _{obs} | 0.120, 0.067 | 0.058, 0.045 |
| wR ₂ _{all} , wR ₂ _{obs} | 0.193, 0.152 | 0.109, 0.102 |
| Δρ _{min,max} (e Å ⁻³) | -0.216, 0.257 | -0.226, 0.234 |

2.3 Virtual Screening The binding efficiencies of the alkyl derivatives were tested *in silico* using docking simulations around the active site of the protein. The known inhibitor SP600125 (537) was docked into the active site of JNK3 to obtain an estimate of its binding energy (-8.05 Kcal/ mol). The predicted binding energies of the other molecules (listed in Table 2 according to increasing length of the alkyl group) were compared with this value. Compared to SP600125, all the derivatives, except **SPM1** and **SPE2**, showed enhanced hydrophobic contacts. With the increase in length of the substituting alkyl group, improved binding energies were observed. It is of interest to note that the binding energies of **SPB1** and **SPB2** are comparable to that of the parent compound and enhanced in case of **SPEN1** and **SPEN2** respectively.

Table 2 Binding energies of 1,9-pyrazoloanthrone derivatives.

| Protein | Ligand | Binding energy eV | Hydrogen Bond between Protein atom and ligand atom | No. of hydrophobic contacts |
|---------|-----------------|-------------------|--|-----------------------------|
| 1PMV | 537 | -8.05 | Met 149 N...N Glu 147 O...N | 9 |
| | SP600125 | | | |
| | SPM1 | -7.70 | Met149 N...O | 7 |
| | SPM2 | -7.80 | Met149 N...O | 11 |
| | SPE1 | -7.87 | Met149 N...O | 9 |
| | SPE2 | -7.90 | Met149 N...O | 11 |
| | SPP1 | -7.88 | Met149 N...O | 11 |
| | SPP2 | -8.09 | Met149 N...O | 13 |
| | SPB1 | -8.11 | Met 149 N...O | 13 |
| | SPB2 | -8.27 | Met 149 N...O | 14 |
| | SPEN1 | -8.61 | Met149 N...O | 11 |
| | SPEN2 | -8.69 | Met149 N...O | 13 |

As described in Fig. 1b the parent molecule 1,9-pyrazoloanthrone in the protein –inhibitor complex interacts with the protein via hydrogen bonds involving the carbonyl oxygen of Glu147 and the main chain nitrogen of Met149. The second hydrogen bonding is conserved in the interactions of all the *N*-alkylated pyrazoloanthrones (ESI†) with the JNK protein (1PMV), as observed from the docking simulations. Fig 3a and 3b show the binding characteristics of **SPB1** and **SPB2** with conserved hydrogen bonding involving MET149. The Ligplot representations of interactions of the other derivatives are presented in ESI†.

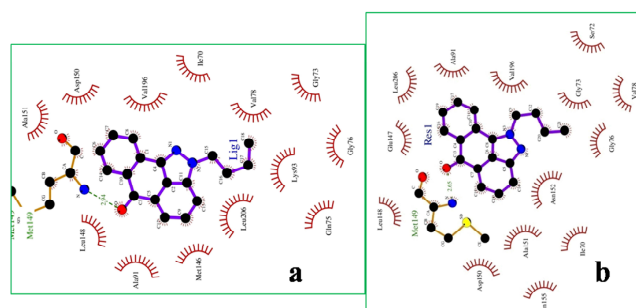


Fig. 3(a) and 3(b) Ligplot representation of interactions in active site of JNK3 with **SPB1** and **SPB2** respectively.

2.4 Biological activity

2.4.1 Evaluation of the biological efficacies of alkyl substituted pyrazoloanthrones.

Sometimes the inhibitor activity of compounds could also be a
 5 result of their toxic effects and consequently might cause a
 flawed conclusion. Hence, prior to utilization of these small
 molecules as inhibitors, the cytotoxic effect of these on
 macrophages at various concentrations has been analyzed by
 MTT (3-(4,5-dimethylthiazol-2-yl)-2,5-diphenyltetrazolium
 10 bromide) assays. All the tested small molecules exhibited

cytotoxic effect greater than 20-30% only beyond 30 μ M
 concentration (Fig. 4). DMSO is utilized in the study as a solvent
 control as it shows no significant cytotoxic effect and helps in
 confirming the specificity of the alkyl derivatives of 1,9-
 15 pyrazoloanthrone in dampening the cell survival. Based on these
 results, the maximum concentration of the pyrazoloanthrone
 derivatives that can be tested for target specific inhibition of JNK
 has been narrowed down to a range of 1 μ M to 30 μ M in further
 studies.

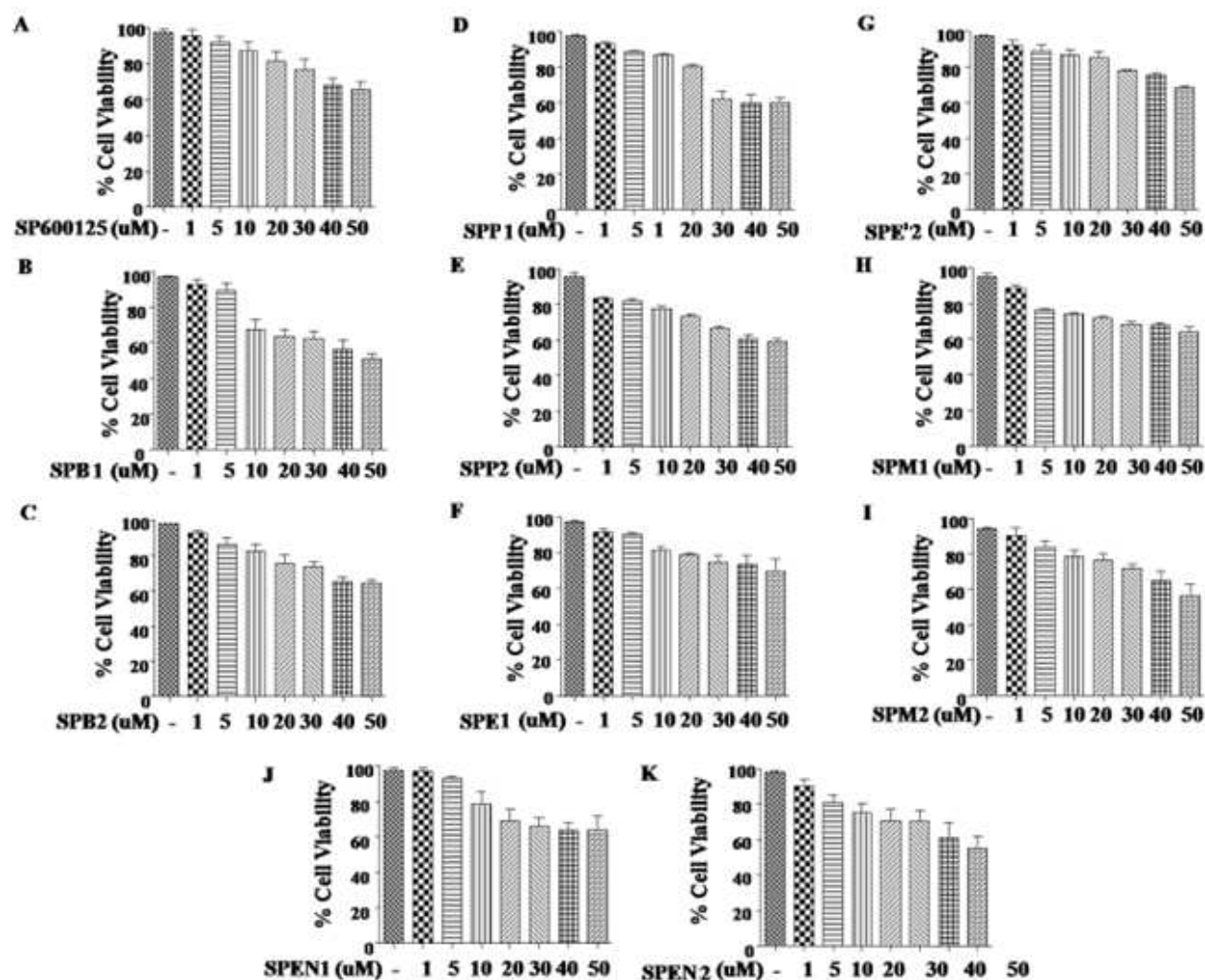


Fig. 4 Analysis of cytotoxic effect of small molecules by MTT assay. Mouse peritoneal macrophages were treated with respective molecules at various concentrations for 12 hours and cell viability was analyzed by MTT assay.

25 Kinase inhibitory effect of alkyl substituted pyrazoloanthrones
 was carried by monitoring the phosphorylation of c-Jun, an
 immediate downstream target of activated JNK in macrophages
 by immunoblotting technique. All the alkyl substituted
 derivatives of pyrazoloanthrone exhibited the inhibition of JNK
 30 over a range of concentrations tested in LPS activated mouse
 macrophages. Of the compounds tested, **SPP1**, **SPB1** and **SPEN1**
 (propyl, butyl and pentyl derivatives of pyrazoloanthrone)
 demonstrated the inhibition of JNK at lower concentrations
 ranging from 1 μ M to 5 μ M whereas 1,9-pyrazoloanthrone showed
 35 inhibition with the minimum requirement of 10 μ M in LPS

activated macrophages as shown in Fig. 5D, E, F and H
 respectively. As reported by Brydon *et al.*, the methyl and ethyl
 derivatives of pyrazoloanthrone showed significant loss in
 inhibitory activity,¹⁹ however, compounds with propyl and butyl
 40 substitutions (**SPP1**, **SPB1** and **SPB2**) showed significant
 inhibitory function starting from 1 μ M whereas **SPEN1** shown
 inhibition from 5 μ M onwards. Intriguingly, all these obtained
 concentrations after the initial screen are far lower as compared to
 1,9-pyrazoloanthrone which initiates inhibition only beyond
 45 10 μ M (Fig. 5H).

Cite this: DOI: 10.1039/c0xx00000x

www.rsc.org/xxxxxx

ARTICLE TYPE

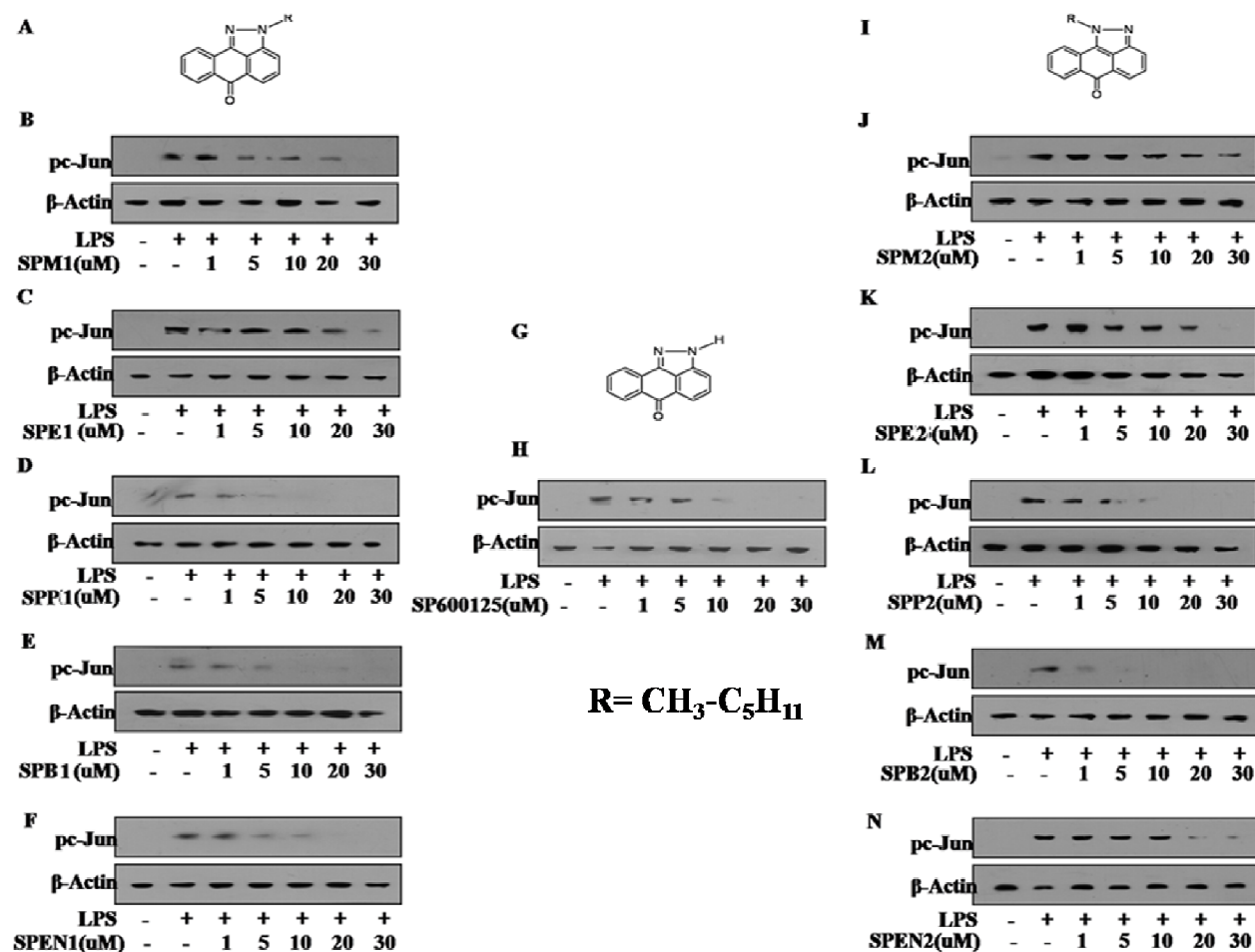


Fig. 5 Optimum inhibitory concentrations of 1, 9-pyrazoloanthrone derivatives over phosphorylation of c-Jun. **B-F** and **J-N** shows the immunoblots for phospho c-Jun in LPS (100ng/ml) activated macrophages at different concentrations of inhibitors tested. **A**, **G** and **I**, represents the structures of 1, 9 pyrazoloanthrone and its derivatives.

Thus, the fact that the substitution of alkyl chains of increasing length enhances the hydrophobic interaction potential which is quite evident from the extent of inhibitory activity with **SPP1** ≈ **SPB1** > **SPEN1** > **SPM1** > **SPE1**. On the other hand, 10 pyrazoloanthrone isomers (derivatives with alkyl substituent on the left side of pyrazole ring) such as **SPP2** (5μM) and **SPB2** (1μM) also showed significant inhibition of JNK activity as well as phosphorylation of c-Jun in comparison to 1,9-pyrazoloanthrone. It is noteworthy that on further extension of 15 chain length like in case of the pentyl derivative of 1,9-pyrazoloanthrone, there is sudden drop in the inhibitory activity and this may be attributed to the requirements of conserved hydrogen bonding at the binding site as demonstrated by the auto dock studies. Interestingly, **SPP1** and **SPB1** exhibited the

20 inhibitory effect at a concentration lower than 1,9-pyrazoloanthrone.

In order to evaluate the specific inhibitory activity of **SPB1** and **SPP1** molecules over JNK compared to other LPS induced 25 activation of other MAPkinases such as ERK1/2 and p38, immunoblot analysis of active state of ERK1/2 and p38 was carried out. **SPP1** and **SPB1** block LPS induced activation of ERK1/2 and p38 only at concentrations beyond 30μM with marginal off target effects. (**Fig. 6**) These results suggest that 30 alkyl substituted pyrazoloanthrone scaffolds needs to be further explored to treat inflammatory disorders with higher specificity at lower concentrations.

Cite this: DOI: 10.1039/c0xx00000x

www.rsc.org/xxxxxx

ARTICLE TYPE

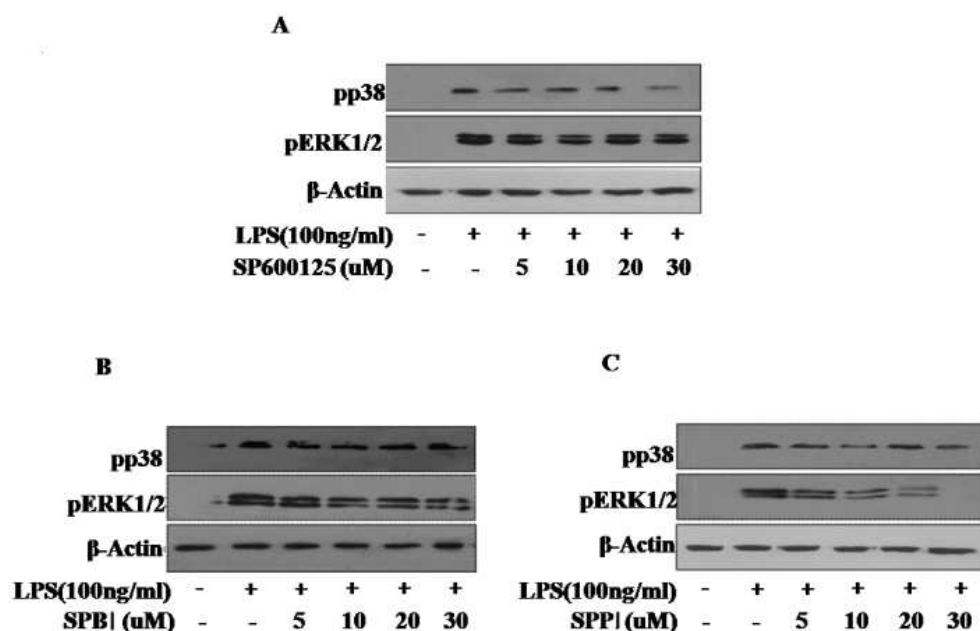


Fig. 6 Elucidation of the off target effect of **SPB1** and **SPP1** over LPS induced MAPkinase activation. **A**, **B** and **C**. Immunoblot analysis of LPS induced activation of p38, ERK1/2 in the presence of various concentrations of SP600125, **SPB1** and **SPP1** respectively in mouse macrophages.

3. Conclusions

In conclusion, the synthesis, isolation and structural determination of alkyl isomers of pyrazoloanthrone derivatives have been achieved. The minimum required inhibitory concentrations of these small molecule inhibitors was found to be less than 10 μM in comparison to 1,9-pyrazoloanthrone to inhibit JNK. The structural correlations appear to support the inhibitor evaluation. The alkyl substituted scaffolds lead to molecules with potent and selective inhibition of JNK. Critically, our lead candidates **SPP1** and **SPB1**, display specific inhibition of JNK among other LPS activated MAP kinases like ERK1/2 and p38. Our results suggest that these two scaffolds of inhibitors **SPP1** and **SPB1** would be promising leads for the further development of more potent and selective inhibitors to treat disorders associated with inflammation.

4. Experimental Section

4.1 Materials and Methods

Isolation of mouse peritoneal macrophages: Macrophages utilized in the study were isolated from C57/BL6J mice. In brief, mice were intraperitoneally injected with thioglycolate (2mL of 2X concentration/mice). After 4 days of injection, mice were sacrificed. Peritoneal cavities were flushed with ice cold PBS and centrifuged to obtain the macrophages. Thus, obtained cells were

resuspended in DMEM containing 10% FBS (Sigma Aldrich) and seeded for further experiments. The experiments with mouse macrophages were carried out after the approval from the Institutional Ethics Committee for animal experimentation as well as from Institutional Biosafety Committee.

4.2 Cell viability assay

Mouse macrophages were seeded in 96 well plates (75,000cells/well) in 200ul of DMEM complete medium and incubated overnight. Later cells were treated with small molecules reconstituted in DMSO at various concentrations as mentioned for 12 hours. Post 12 hour treatment, medium was removed carefully and fresh medium (100ul/well) was added. 20ul of 5mg/ml of MTT reagent was added to each well and incubated for 4 hours at 37°C aseptically. Medium was removed and cells were added with DMSO (100ul/well) and left on orbital shaker (150rpm) 15min. After incubation, absorbance was read at 590nm. Untreated cells served as control in all the cell viability assays.

4.3 Treatment with small molecule inhibitors

All the small molecules utilized in the study were reconstituted in sterile DMSO (Sigma-Aldrich, USA) and used at various concentrations as mentioned. DMSO at 0.1% concentration was used as the vehicle control. In all experiments with inhibitors, a tested concentration was used after careful titration experiments

assessing the viability of the macrophages using MTT assay. In experiments with inhibitors, the cells (4×10^6 /well) were treated with a given inhibitor for 60 min before experimental treatment.

4.4 Immunoblotting

Macrophages were treated with respective small molecule inhibitor as mentioned and then stimulated with LPS (Sigma-Aldrich, USA), 100ng/ml, for additional 60min. Cells were washed twice with PBS, scrapped off the culture dish and collected by centrifugation. Cell lysates were prepared in RIPA buffer constituting 50mM Tris-HCl (pH 7.4), 1% NP-40, 0.25% Sodium deoxycholate, 150mM NaCl, 1mM EDTA, 1mM PMSF, 1µg/ml of each aprotinin, leupeptin, pepstatin, 1mM Na_3VO_4 , 1mM NaF and incubated in ice for 30min. Whole cell lysates were collected by centrifuging lysed cells at 13,000 RPM, 10min at 4°C. Equal amount of protein from each cell lysate was subjected to SDS-PAGE and transferred onto PVDF membranes (Millipore, USA) by semidry western blotting (Bio-Rad, USA) method. Nonspecific binding was blocked with 5% nonfat dry milk powder in TBST (20mM Tris-HCl (pH 7.4), 137mM NaCl, and 0.1% Tween 20) for 60 min. The blots were probed with anti phospho Ser 63 c-Jun for 12 hours at 4°C and then washed with TBST thrice followed by anti rabbit IgG HRP conjugated secondary antibody for 2 hours at 4°C. Blots were washed and developed using enhanced chemiluminescence detection system (Perkin Elmer, USA) as per manufacturer's instructions. Blots were probed with anti-β-actin HRP (Sigma-Aldrich, USA) to ensure equal loading of protein.

4.5 Docking

The three-dimensional (3D) structures of all ten small molecules were modelled and minimised using the PRODRG server³¹ and single crystal structures. AutoDock (version 4.2)³² was used for the ligand-protein docking. The Lamarckian Genetic Algorithm was used with a population of 200 dockings. The docking output was analysed using Pymol and Ligplot³³. Hydrogen bonds were determined using the in-built HBPLUS³⁴ module in Ligplot with hydrogen bonding parameters ($\text{D} \cdots \text{A}$ distance $\leq 3.35 \text{ \AA}$, $\text{H} \cdots \text{A} \leq 2.7 \text{ \AA}$).

Abbreviations

| | |
|-----------|--|
| c-JNK | c-Jun N-terminal Kinase |
| MAPKinase | Mitogen Activated Protein Kinase |
| LPS | Lipopolysaccharide |
| ERKs | Extracellular signal-regulated kinases |

Acknowledgements

Authors thank Indian Institute of Science for infrastructure facilities and financial support. We thank the Central Animal facility, Indian Institute of Science for providing mice for experimentation. KDP and JT acknowledge fellowships from CSIR (Council of Scientific Industrial research). TNG thanks DST for J C Bose fellowship.

^a Solid state and structural chemistry unit, Indian Institute of science, Bangalore, India. Fax: +91(0) 80 2360 1310; Tel: +91(0) 80 22932796;

^b Department of Microbiology and Cell Biology, Indian Institute of science, Bangalore, India. Fax: +91-80-23602697; Tel: +91-80-2293 3223;

^c Department of Physics, Indian Institute of Science, Bangalore, India.

^d Supercomputer Education and Research Centre, Indian Institute of science, Bangalore, India.

[#] Corresponding Authors: E-mail: sctng@sscu.iisc.ernet.in;

balaji@mcbli.iisc.ernet.in

† Electronic Supplementary Information (ESI) available: Crystal structures, NMR and ligplots. See DOI: 10.1039/b000000x/

‡ CCDC numbers: **SPE2**-990062; **SPP1**-990060; **SPP2**-990061; **SPB1**-990059; **SPB2**-990535.

References

- D. C. Angus and T. V. Poll, *N Engl J Med*, 2013, **369**, 2062-2063.
- N. A. Ali, *Crit Care*, 2010, **14**, 160.
- J. Moreira, *N Engl J Med.*, 2013, **369**, 2062-2063.
- W. J. Lin and W. C. Yeh, *Shock*, 2005, **24**, 206-209.
- N. Mukaida, Y. Ishikawa, N. Ikeda, N. Fujioka, S. Watanabe, K. Kuno and K. Matsushima, *J Leukoc Biol*, 1996, **59**, 145-151.
- K. Watanabe, H. Nakagawa and S. Tsurufuji, *Agents Actions* 1986, **17**, 472-477.
- R. M. Pinheiro and J. B. Calixto, *Inflamm Res* 2002, **51**, 603-610.
- M. S. Inayat, I. S. El-Amouri, M. Bani-Ahmad, H. L. Elford, V. S. Gallicchio and O. R. Oakley, *J Inflamm (Lond)*, **2013**, **7**, 43.
- T. Kallunki, B. Su, I. Tsigelny, H. K. Sluss, B. Derijard, G. Moore, R. Davis and M. Karin, *Genes Dev* 1994, **8**, 2996-3007.
- B. Derijard, M. Hibi, I. H. Wu, T. Barrett, B. Su, T. Deng, M. Karin and R. J. Davis, *Cell* 1994, **76**, 1025-1037.
- M. A. Bogoyevitch and P. G. Arthur, *Biochim Biophys Acta* 2008, **1784**, 76-93.
- M. Karin, *J Biol Chem* 1995, **270**, 16483-6.
- G. McMahon, L. Sun, C. Liang and C. Tang, *Curr Opin Drug Discov Devel* 1998, **1**, 131-146.
- V. C. Foletta, D. H. Segal and D. R. Cohen, *J Leukoc Biol* 1998, **63**, 139-152.
- J. Jain, V. E. Valge-Archer, A. Rao, *J Immunol* 1992, **148**, 1240-1250.
- S. Gupta, T. Barrett, A. J. Whitmarsh, J. Cavanagh, H. K. Sluss, B. Derijard and R. J. Davis, *EMBO J* 1996, **15**, 2760-2770.
- P. P. Graczyk, *Future Med Chem*, 2013, **5**, 539-51,
- Z. Xia, M. Dickens, J. Raingeaud, R. J. Davis and M. E. Greenberg, *Science* 1995, **270**, 1326-1331.
- B. L. Bennett, D. T. Sasaki, B. W. Murray, E. C. O'Leary, S. T. Sakata, W. Xu, J. C. Leisten, A. Motiwala, S. Pierce, Y. Satoh, S. S. Bhagwat, A. M. Manning and D. W. Anderson, *Proc Natl Acad Sci U S A* 2001, **98**, 13681-13686.
- A. Cerbone, C. Toaldo, S. Pizzimenti, P. Pettazoni, C. Dianzani, R. Minelli, E. Ciamporcerio, G. Roma, M. U. Dianzani, R. Canaparo, C. Ferretti and G. Barrera, *PPAR Res*, 2012, 269751.
- T. Kamenecka, R. Jiang, X. Song, D. Duckett, W. Chen, Y. Y. Ling, J. Habel, J. D. Laughlin, J. Chambers, M. Figueroa-Losada, M. D. Cameron, L. Lin, C. H. Ruiz and P. V. LoGrasso, *J Med Chem*, 2010, **53**, 419-431.
- N. Kwiatkowski, N. Jelluma, P. Filippakopoulos, M. Soundararajan, M. S. Manak, M. Kwon, H. G. Choi, T. Sim, Q. L. Deveraux, S. Rottmann, D. Pellman, J. V. Shah, G. J. Kops, S. Knapp and N. S. Gray, *Nat Chem Biol*, 2010, **6**, 359-368.
- M. A. Siddiqui and P. A. Reddy, *J Med Chem*, 2010, **53**, 3005-3012.
- H. D. Showalter, J. L. Johnson, J. M. Hoftiezer, W. R. Turner, L. M. Werbel, W. R. Leopold, J. L. Shillis, R. C. Jackson and E. F. Elslager, *J Med Chem* 1987, **30**, 121-131.
- K. D. Prasad, N. Venkataramaiah, and T. N. Guru Row, *Cryst. Growth Des.*, 2014, DOI:10.1021/cg5002489
- K. Assi, R. Pillai, A. Gomez-Munoz, D. Owen and B. Salh, *Immunology* 2006, **118**, 112-121.
- Y. T. Ip and R. J. Davis, *Curr Opin Cell Biol* 1998, **10**, 205-219.
- N. Miyakoshi, C. Richman, Y. Kasukawa, T. A. Linkhart, D. J. Baylink and S. Mohan, *J Clin Invest* 2001, **107**, 73-81.

- 29 L. Havlíčková, A. Koloničný, A. Lyčka, J. Jirman and I. Kolb, *Dyes and pigments*, 1989, **10**, 1-11.
- 30 G. Scapin, S. B. Patel, J. Lisnock, J. W. Becker and P. V. LoGrasso, *Chemistry & biology*, 2003, **10**, 705-712.
- 5 31 A.W. Schuttelkopf and D. M. F. Van Aalten, , PRODRG - a tool for high-throughput crystallography of protein-ligand complexes. *Acta Crystallogr. D*, 2004, **60**, 1355-1363.
- 32 G.M. Morris, R. Huey, W. Lindstrom, M. F. Sanner, R. K. Belew, D. S. Goodsell and A. J. Olson, AutoDock4 and AutoDockTools4: automated docking with selective receptor flexibility, *J. Computational Chemistry*. 2009, 2785-2791.
- 10 33 A.C. Wallace, R. A. Laskowski, and J. M. Thornton, LIGPLOT: A program to generate schematic diagrams of protein-ligand interactions. *Prot. Eng.*, 1995, **8**, 127-134.
- 15 34 I.K. McDonald, and J. M. Thornton, *J. Mol. Biol.*, 1994, **238**, 777-793.